Generalized Fractional Matched Filtering and its Applications

Peeyush Sahay
Department of Electrical Engineering
IIT Bombay
Mumbai, India
sahay.peeyush@gmail.com

Ameya Anjarlekar
Department of Electrical Engineering
IIT Bombay
Mumbai, India
ameyanjarlekar@gmail.com

Shubham Anand Jain
Department of Electrical Engineering
IIT Bombay
Mumbai, India
shubhamjainiitb@gmail.com

P. Radhakrishna
LRDE
DRDO
Bangalore, India
prk@lrde.drdo.in

Vikram M. Gadre
Department of Electrical Engineering
IIT Bombay
Mumbai, India
vmgadre@ee.iitb.ac.in

***Abstract*—Time domain matched filtering is a classic method used in radar and sonar applications to maximize signal to noise ratio (SNR) gain, estimate time delay, and improve range resolution. Fractional Fourier transform, and fractional Fourier domain matched filtering are used extensively to overcome the drawbacks of time domain matched filtering and are shown to have improved performance for a linear chirp. This paper presents a generalized fractional matched filtering (GFMF) for estimating higher order chirp parameters with known time delay. It is shown to provide SNR gain equivalent to time domain matched filtering. As an application of GFMF, a novel method to minimize SNR gain degradation due to the range-Doppler coupling effect of quadratic chirps is presented. For a higher order chirp with unknown time delay, another method using generalized fractional envelope correlator (GFEC) is proposed, which performs joint estimation of time delay and higher order chirp parameters using a double quadratic chirp.**

***Index Terms*—Higher order chirp, fractional matched filtering, parameter estimation, fractional envelope correlation.**

I. Introduction

Time domain matched filtering correlates a known signal (replica of the transmitted signal) with an unknown signal (received signal) [1]. Time domain matched filter gives the highest SNR gain, improves range resolution, and is useful for estimating time delay of high SNR as well as low SNR moving targets in radar and sonar applications. In the case of linear and higher order chirps, time domain matched filtering produces significant degradation in output SNR due to the range-Doppler coupling, and is unable to estimate higher order chirp parameters [2, pp. 803-806].

The fractional Fourier matched filter was proposed for linear chirps, and it was shown to perform better than time-domain matched filtering in the presence of chirp noise [1]. FrFT (fractional Fourier transform) and FrFT domain matched filtering also provide better sidelobe suppression as compared to time-domain matched filtering for linear chirps [3], [4]. FrFT performs better than time-domain matched filtering for linear chirps in the presence of Doppler frequency because its peak amplitude depends on the chirp rate.

The second section of this paper describes the basics of generalized time-frequency transform (GTFT). The third section of this paper describes GTFT based matched filter called GFMF, which generalizes fractional and time domain matched filtering. Its SNR gain is shown to be comparable to time domain matched filtering for higher order chirps. It also describes applications of GFMF to solve SNR gain degradation due to the range-Doppler coupling effect in quadratic chirps.

GFMF estimates higher order chirp parameters with known time delay. But in case of unknown time delay, joint time delay and higher order chirp offset parameter estimation is an important issue in signal processing and well-known problem in wireless communication systems [5], [6]. Joint estimation of time delay and frequency offset was proposed using sum of two linear chirps waveform by fractional Fourier envelope correlator [5]. Fractional Fourier envelope correlation provides good target detection in case of low SNR, and it gives superior noise performance compared to FrFT [5]. Joint estimation of time delay, frequency offset, and frequency offset rate was proposed for the detection of passive systems by cross-ambiguity function [6]. However, it cannot be used for detecting higher order frequency offset parameters. This paper proposes a novel method for joint estimation of time delay and higher order chirp offset parameters using GFEC and double quadratic chirp, described in the fourth section of the paper. It also describes mean square error (MSE) simulations for joint parameter estimation of time-delayed higher order chirp.

II. Basics of GTFT

If a signal $x(t)$ has finite absolute integral (finite L^1 norm), its GTFT evaluated at parameters (α, λ) is given by

$$X_{\alpha,\lambda}(f) = \int_{-\infty}^{+\infty} x(t) K_{\alpha,\lambda}(t, f) dt, \qquad (1)$$

where $K_{\alpha,\lambda}(t,f)$ is kernel of GTFT and defined as [7]

$$K_{\alpha,\lambda}(t,f)=\begin{cases}\sqrt{1-i\cot\alpha}\cdot exp\Big(i\pi t_0^2 f^2\cot\alpha+i\pi f_0^2 t^2\cot\alpha-i2\pi ft\\ \text{cosec}\alpha+i\cdot h(\lambda,t_0 f)-i\cdot h(\lambda,f_0 t)\Big), \text{if } \alpha\neq n\pi\\ \delta(f_0t-t_0f), & \text{if } \alpha=2n\pi\\ \delta(f_0t+t_0f), & \text{if } \alpha=(2n+1)\pi\end{cases}$$

where $h(\cdot)$ is a real valued dimensionless function, n is an integer, α and λ are real valued GTFT parameters, t_0 (in seconds), f_0 (in Hertz) are dimensional normalisation factors, $t_0^2=\frac{T_{max}}{f_s}$, $f_0^2=\frac{f_s}{T_{max}}$, $t_0^2f_0^2=1$, T_{max} is the window length during GTFT and f_s is the sampling frequency.

The GTFT can be used to analyze a much wider variety of frequency modulated signals by varying $h(\cdot)$ in the GTFT kernel. Cubic-kernel-GTFT (ck-GTFT) may be defined by substituting the parametric function $h(\cdot)$ as

$$h(\lambda,z)=\pi\lambda z^3. \tag{2}$$

It is to be noted that ck-GTFT is similar to third order polynomial Fourier transform, with the added advantage of possessing the property of index additivity of angle.

III. Generalized fractional matched filter

This section presents the mathematical derivation of maximum SNR gain and impulse response of GFMF.

A. Maximum SNR gain and impulse response of GFMF

Let $S_{\alpha,\lambda}(f_{\alpha,\lambda})$ represent the GTFT domain power spectral density at (α,λ) for input time domain additive white Gaussian noise (AWGN), where α and λ are parameters of ck-GTFT kernel. GTFT domain power spectrum density is a generalization of the fractional power spectral density [8]. Let $H_{\alpha,\lambda}(f_{\alpha,\lambda})$ be the transfer function of the matched filter in GTFT domain at parameters (α,λ).
Output noise power spectral density $S^{out}_{\alpha,\lambda}(f_{\alpha,\lambda})$ at (α,λ) is given by $S^{out}_{\alpha,\lambda}(f_{\alpha,\lambda})=|H_{\alpha,\lambda}(f_{\alpha,\lambda})|^2\cdot S_{\alpha,\lambda}(f_{\alpha,\lambda})$.

Thus, total output noise power at $(\alpha,\lambda)=\int_{-\infty}^{+\infty}S^{out}_{\alpha,\lambda}(f_{\alpha,\lambda})df_{\alpha,\lambda}$.

From conservation of energy along any angle in GTFT,

$$\int_{-\infty}^{+\infty}S^{out}_{\alpha,\lambda}(f_{\alpha,\lambda})df_{\alpha,\lambda}=\int_{-\infty}^{+\infty}S^{out}_{\alpha+\pi/2,\lambda}(f_{\alpha+\pi/2,\lambda})df_{\alpha+\pi/2,\lambda}. \tag{3}$$

Let $X_{\alpha,\lambda}(f_{\alpha,\lambda})$, $Y_{\alpha,\lambda}(f_{\alpha,\lambda})$ be the input and the output of the GFMF at parameters (α,λ) respectively. If $SNR^{out}_{\alpha,\lambda}$ is output SNR of GFMF at (α,λ), then we have

$$SNR^{out}_{\alpha,\lambda}=\frac{\text{Peak signal power in GTFT domain at }(\alpha,\lambda)}{\text{Total noise power in GTFT domain at }(\alpha,\lambda)}.$$

The output signal $Y_{\alpha,\lambda}(f_{\alpha,\lambda})$ at (α,λ) is given by $F^{\frac{-\pi}{2}}\left[X_{\alpha+\frac{\pi}{2},\lambda}(f_{\alpha+\frac{\pi}{2},\lambda})\cdot H_{\alpha+\frac{\pi}{2},\lambda}(f_{\alpha+\frac{\pi}{2},\lambda})\right]$, where $F^{\frac{-\pi}{2}}$ is the inverse Fourier transform operator. Assume $\alpha+\pi/2=\beta$, then the output SNR of the GFMF is:

$$SNR^{out}_{\alpha,\lambda}=\frac{max\left|\int_{-\infty}^{\infty}X_{\beta,\lambda}(f_{\beta,\lambda})H_{\beta,\lambda}(f_{\beta,\lambda})e^{i2\pi f_{\alpha,\lambda}f_{\beta,\lambda}}df_{\beta,\lambda}\right|^2}{\int_{-\infty}^{\infty}S_{\beta,\lambda}(f_{\beta,\lambda})|H_{\beta,\lambda}(f_{\beta,\lambda})|^2df_{\beta,\lambda}}, \tag{4}$$

Let numerator be highest at $f_{\alpha,\lambda}=f'_{\alpha,\lambda}$, then output SNR is

$$SNR^{out}_{\alpha,\lambda}=\frac{\left|\int_{-\infty}^{\infty}\frac{X_{\beta,\lambda}(f_{\beta,\lambda})\sqrt{S_{\beta,\lambda}(f_{\beta,\lambda})}}{\sqrt{S_{\beta,\lambda}(f_{\beta,\lambda})}}H_{\beta,\lambda}(f_{\beta,\lambda})e^{i2\pi f'_{\alpha,\lambda}f_{\beta,\lambda}}df_{\beta,\lambda}\right|^2}{\int_{-\infty}^{\infty}S_{\beta,\lambda}(f_{\beta,\lambda})|H_{\beta,\lambda}(f_{\beta,\lambda})|^2df_{\beta,\lambda}}. \tag{5}$$

From Cauchy-Schwartz inequality, we get

$$SNR^{out}_{\alpha,\lambda}\leq\left[\int_{-\infty}^{\infty}\frac{|X_{\beta,\lambda}(f_{\beta,\lambda})|^2}{S_{\beta,\lambda}(f_{\beta,\lambda})}df_{\beta,\lambda}\right]. \tag{6}$$

$$\text{Thus, maximum } SNR^{out}_{\alpha,\lambda}=\int_{-\infty}^{\infty}\frac{|X_{\beta,\lambda}(f_{\beta,\lambda})|^2}{S_{\beta,\lambda}(f_{\beta,\lambda})}df_{\beta,\lambda}. \tag{7}$$

Let $n(t)$ be time domain AWGN with power spectrum density $\frac{\eta}{2}$ and E is expectation operator in GTFT frequency domain. Then, the GTFT domain power spectral density of $n(t)$ at parameters (β,λ) can be written as:

$$\begin{aligned}S_{\beta,\lambda}(f_{\beta,\lambda})&=E\left[\left|\int n(\tau)K_{\beta,\lambda}(\tau,f_{\beta,\lambda})d\tau\right|^2\right],\\ &=\int\int\int n(\tau_1)n^*(\tau_2)K_{\beta,\lambda}(\tau_1,f_{\beta,\lambda})\\ &\qquad K^*_{\beta,\lambda}(\tau_2,f_{\beta,\lambda})d\tau_1d\tau_2df_{\beta,\lambda},\\ &=\int\int\int n(\tau_1)n^*(\tau_2)|\text{cosec}\beta|exp[i\pi\cot\beta\\ &\quad\cdot f_0^2(\tau_1^2-\tau_2^2)+i2\pi f_{\beta,\lambda}\text{cosec}\beta(\tau_2-\tau_1)\\ &\quad+i\cdot h(\lambda,f_0\tau_2)-i\cdot h(\lambda,f_0\tau_1)]d\tau_1d\tau_2df_{\beta,\lambda}.\end{aligned}$$

$$S_{\beta,\lambda}(f_{\beta,\lambda})=\int|n(\tau)|^2d\tau=\frac{\eta}{2}. \tag{8}$$

From conservation of energy along any angle in GTFT, $\int_{-\infty}^{\infty}|X_{\beta,\lambda}(f_{\beta,\lambda})|^2df_{\beta,\lambda}=\tau$, where τ is pulse width. The input noise power spectrum density at β in Eq. (8) is substituted in Eq. (7) to get the expression for maximum $SNR^{out}_{\alpha,\lambda}$. After these substitution in Eq. (7), maximum $SNR^{out}_{\alpha,\lambda}=2\cdot\tau/\eta$. Considering a unit amplitude signal, we get

$$\begin{aligned}\text{GFMF SNR gain at }(\alpha,\lambda)&=\frac{\text{Maximum }SNR^{out}_{\alpha,\lambda}}{SNR^{in}_{\alpha,\lambda}},\\ &=\frac{2\cdot\tau/\eta}{2/\eta}=\tau,\end{aligned} \tag{9}$$

where $SNR^{in}_{\alpha,\lambda}$ is the input SNR at (α,λ), and $SNR^{in}_{\alpha,\lambda} = \frac{1}{\eta/2}$. Thus, the SNR gain of GFMF at (α,λ) is equal to time domain matched filter, as demonstrated in Eq. (9). Equality holds in Eq. (6) when,

$$\left[\frac{X_{\beta,\lambda}(f_{\beta,\lambda})}{\sqrt{S_{\beta,\lambda}(f_{\beta,\lambda})}}\right]^* = k.\left[\sqrt{S_{\beta,\lambda}(f_{\beta,\lambda})} \cdot H_{\beta,\lambda}(f_{\beta,\lambda}) e^{i2\pi f'_{\alpha,\lambda} f_{\beta,\lambda}}\right], \quad (10)$$

where k is a real constant and * is the conjugate operator.

$$H_{\beta,\lambda}(f_{\beta,\lambda}) = \frac{X^*_{\beta,\lambda}(f_{\beta,\lambda}) \cdot e^{-i2\pi f'_{\alpha,\lambda} f_{\beta,\lambda}}}{k.S_{\beta,\lambda}(f_{\beta,\lambda})}. \quad (11)$$

Now, from Eq. (11), by taking inverse Fourier transform we get the impulse response of GFMF at (α,λ) as:

$$H_{\alpha,\lambda}(f_{\alpha,\lambda}) = \frac{2X^*_{\alpha,\lambda}(f'_{\alpha,\lambda} - f_{\alpha,\lambda})}{k \cdot \eta}. \quad (12)$$

Without loss of generality we can assume $k = 1$ (as k is a proportionality constant) and $f'_{\alpha,\lambda} = 0$. Then, we get

$$H_{\alpha,\lambda}(f_{\alpha,\lambda}) = \frac{2X^*_{\alpha,\lambda}(-f_{\alpha,\lambda})}{\eta}. \quad (13)$$

When $\lambda = 0$, from Eq. (13), then impulse response of GFMF becomes impulse response of fractional Fourier matched filter [3]. When $\lambda = 0$ and $\alpha = \frac{\pi}{2}$, then impulse response of GFMF becomes transfer function of time domain matched filter.

B. Simulation results: SNR gain comparison of GFMF

In this section, Monte Carlo simulation of 500 iterations has been performed to compare SNR gain of GFMF with SNR gain of time domain matched filtering, FrFT, and GTFT for a single quadratic chirp. Fig. (1) shows the SNR gain comparison in the presence of AWGN noise and zero Doppler frequency of quadratic chirp.

As shown in Fig. (1), SNR gain of GFMF is equal to SNR gain of time domain matched filtering, and this corroborates the mathematical derivation in Eq. (9). GFMF is useful as compared to time domain matched filtering, as it gives equivalent SNR gain and is able to estimate higher order chirp parameters. SNR gain of GTFT is less than GFMF. SNR gain of FrFT is less than GTFT and GFMF due to the presence of the quadratic phase. GFMF outperforms time domain matched filtering, FrFT, and GTFT in terms of SNR gain and estimating higher order chirp parameters with known time delay. For chirps with unknown time delay, we propose another method in the fourth section of this paper.

The parameters for the simulation are pulse width = 1 sec, SNR variation = (0:10:40) dB, chirp rate = 100 Hz^2, quadratic rate = 150 Hz^3, time delay = 0 sec.

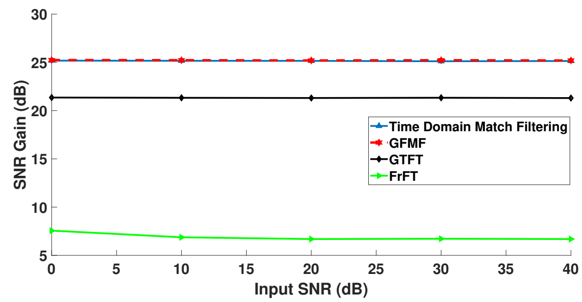

Fig. 1. SNR gain comparison at 0 Hz Doppler frequency

C. GFMF applications: Range-Doppler coupling effect

In this section, Monte Carlo simulation of 500 iterations has been performed to compare SNR gain degradation of time domain matched filtering with GFMF for a single quadratic chirp. Time-domain matched filtering gives SNR gain degradation due to a significant mismatch between the transmitted and received waveforms in the case of linear chirp and higher order chirp. When the Doppler frequency of the received waveform is large with respect to waveform bandwidth, then time-domain matched filtering produces significant degradation in output SNR [2, pp. 803-806]. The simulation shown in Fig. (2) compares the SNR gain of GFMF and time domain matched filtering with varying Doppler frequency. Similar simulation parameters as the previous simulation are considered, and Doppler frequency varied with the percentage of signal bandwidth, denoted as percentage fractional Doppler shift. In the simulation, SNR gain of time domain matched filtering decreases with an increase in Doppler frequency. SNR gain in GFMF is almost constant with respect to Doppler frequency because the peak amplitude of GFMF depends on α and λ parameters of GTFT kernel and is independent of Doppler frequency. Hence, GFMF is capable of solving SNR gain degradation due to the range-Doppler coupling effect in quadratic chirps.

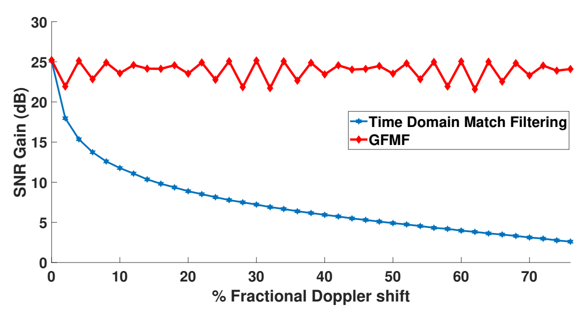

Fig. 2. SNR gain variation w.r.t percentage fractional Doppler shift

IV. Generalized Fractional Envelope Correlation

In the case of GFMF, for quadratic chirps, peak amplitude's position depends on α parameter of GTFT kernel, which in turn depends on time delay. Since quadratic chirp contains third order phase terms, a closed-form expression for a peak position of GFMF output is difficult to determine. Hence, this section presents GFEC, which is a generalization of fractional envelope correlator [5]. GFEC is a method to determine time delay and perform joint estimation of higher order chirp offset parameters in case of unknown time delay.

A. Calculation of peak shift

This subsection presents the calculation of the peak position of GFEC output for a quadratic chirp.

1) ck-GTFT of the transmitted chirp pulse: Consider a quadratic chirp transmission waveform $x^{tr}(t)$ as:

$$x^{tr}(t) = rect\left(\frac{t}{\tau}\right) e^{ia\pi t^2 + ic\pi t^3}, \tag{14}$$

where a is chirp rate and c is quadratic rate. We define λ^o and α^o to be corresponding λ and α at matched conditions respectively. Also, $X^{tr}_{\alpha_1^o,\lambda_1^o}(f)$ is the corresponding GTFT transform of $x^{tr}(t)$ at matched conditions. Thus, at matched GTFT of cubic phase, $c - f_0^3\lambda_1^o = 0$, quadratic phase $f_0^2 \cot\alpha_1^o + a = 0$, and putting $A_{\alpha_1^o} = \sqrt{\text{cosec}\alpha_1^o}$, we get

$$|X^{tr}_{\alpha_1^o,\lambda_1^o}(f)| = A_{\alpha_1^o}\tau \cdot sinc(f_{\alpha_1^o,\lambda_1^o} \cdot \text{cosec}\alpha_1^o \cdot \tau). \tag{15}$$

2) ck-GTFT of the received pulsed chirp waveform: Considering an extension of the echo model presented in [6], the received signal $x^{recv}(t)$ is taken to be:

$$\begin{aligned} x^{recv}(t) &= x(t-t_d).e^{i2\pi f_d t + i\pi a_r t^2 + i\pi J_r t^3}, \\ &= rect\left[\frac{t-t_d}{\tau}\right] e^{ic\pi(t-t_d)^3 + ia\pi(t-t_d)^2} \\ &\quad \cdot e^{i2\pi f_d t + i\pi a_r t^2 + i\pi J_r t^3}, \end{aligned} \tag{16}$$

where t_d is time delay, f_d is frequency offset, a_r is frequency offset rate, and J_r is rate of frequency offset rate. Also, $X^{recv}_{\alpha_1^o,\lambda_1^o}(f)$ is the corresponding GTFT transform of $x^{recv}(t)$ at matched conditions. At matched cubic phase $(c+J_r) - f_0^3\lambda_2^o = 0$, quadratic phase $f_0^2\cot\alpha_2^o + a + a_r - 3ct_d = 0$, and putting $A_{\alpha_2^o} = \sqrt{\text{cosec}\alpha_2^o}$ we get

$$|X^{recv}_{\alpha_2^o,\lambda_2^o}(f)| = A_{\alpha_2^o}\tau sinc(\tau[f\text{cosec}\alpha_2^o - f^p]), \tag{17}$$

where $f^p = 1.5ct_d^2 - at_d + f_d$. Further, substituting quadratic matched conditions, $a = 3ct_d - a_r - f_0^2\cot\alpha_2^o$ of the received signal in the expression of f^p we obtain,

$$f^p = f_0^2 t_d \cot\alpha_2^o + f_d - 1.5ct_d^2 + a_r t_d, \tag{18}$$

3) Envelope correlation in GTFT domain: GTFT of transmit wave at parameters $(\alpha_1^o, \lambda_1^o)$ is taken from Eq. (15), and GTFT of the received wave at parameters $(\alpha_2^o, \lambda_2^o)$ is taken from Eq. (17). In this method, cross correlation of known transmitted waveform and the unknown received waveform is performed, without considering the phase component. We choose the chirps such that $|\sin\alpha_2^o| > |\sin\alpha_1^o|$. Using Eq. (15) and Eq. (17), we formulate GFEC correlated output $X^{corr}(\epsilon)$, which can be written as a multiplication in the Fourier domain.

$$\begin{aligned} X^{corr}(\epsilon) &= F^{\frac{\pi}{2}}\left[F^{\frac{-\pi}{2}}[|X^{recv}(f)|] \cdot F^{\frac{-\pi}{2}}[|X^{tr}(f)|]\right], \\ &= F^{\frac{\pi}{2}}\left[\frac{A_{\alpha_1^o}}{\text{cosec}\alpha_1^o} \cdot rect\left[\frac{t}{\tau\text{cosec}\alpha_1^o}\right] \cdot \frac{A_{\alpha_2^o}}{\text{cosec}\alpha_2^o} \cdot \right. \\ &\quad \left. rect\left[\frac{t}{\tau\text{cosec}\alpha_2^o}\right] exp\left(i2\pi t\sin\alpha_2^o f^p\right)\right], \\ &= A_{\alpha_1^o}A_{\alpha_2^o}\tau\sin\alpha_1^o sinc(\tau\cdot[f\cdot\text{cosec}\alpha_2^o - f^p]). \end{aligned} \tag{19}$$

The correlation of two shifted, unequal sinc waveforms in the GTFT domain is a sinc waveform. The peak shift would be equal to the offset of frequencies between the sinc waveforms. Thus, the peak shift in GFEC output is given by: $f^p \cdot \sin\alpha_2^o$. For simplicity of notation, we henceforth replace α_2^o by α. Thus, we get that:

$$\Delta d = f_0^2 t_d\cos\alpha + f_d\sin\alpha - 1.5ct_d^2\sin\alpha + a_r t_d\sin\alpha, \tag{20}$$

where Δd is peak shift of output of GFEC. After normalization, the samples are spaced $\frac{1}{\Delta x} = \frac{1}{\sqrt{T_{max}\cdot f_s}}$ apart in GTFT domain; so to get the actual sample difference, we have to multiply distance Δd with Δx and t_0. After performing dimensional normalization in GTFT domain, expression of peak shift of output of GFEC can be given by:

$$\Delta d_n = \Delta x\Delta d\cdot t_0, \tag{21}$$

$$\begin{aligned} &= \left[\sqrt{T_{max}f_s}\right]\cdot\sqrt{\frac{T_{max}}{f_s}}\left[t_d\cos\alpha\cdot\frac{f_s}{T_{max}} + f_d\sin\alpha\right. \\ &\quad \left. - 1.5c\cdot t_d^2\sin\alpha + a_r\cdot t_d\sin\alpha\right], \end{aligned} \tag{22}$$

$$= f_s t_d\cos\alpha + (f_d - 1.5ct_d^2 + a_r t_d)T_{max}\sin\alpha, \tag{23}$$

where Δd_n is peak shift of output of GFEC after dimensional normalization. Hence, the peak shift is given by:

$$\Delta d_n = f_s t_d\cos\alpha + (f_d - 1.5ct_d^2 + a_r t_d)T_{max}\sin\alpha \tag{24}$$

B. GFEC applications: Joint parameter estimation

This section presents the mathematical derivation for joint estimation of time delay and chirp offset parameter. The transmitted signal $x^{tr}(t)$ is a double quadratic chirp, used for joint parameter estimation. A double quadratic chirp contains two quadratic chirps of the same pulse width but different chirp parameters, and is given by:

$$x^{tr}(t) = rect\left(\frac{t}{\tau}\right).[e^{ic_1\pi t^3 + ia_1\pi t^2} + e^{ic_2\pi t^3 + ia_2\pi t^2}], \tag{25}$$

Considering an extension of the echo model presented in [6], the received signal $x^{recv}(t)$ is given by:

$$\begin{aligned} x^{recv}(t) &= x(t-t_d).e^{i2\pi f_d t + i\pi a_r t^2 + i\pi J_r t^3}, \\ &= rect\left[\frac{t-t_d}{\tau}\right]\cdot\left[e^{ic_1\pi(t-t_d)^3 + ia_1\pi(t-t_d)^2}\right. \\ &\quad \left. + e^{i.c_2\pi(t-t_d)^3 + ia_2\pi(t-t_d)^2}\right]\cdot e^{i2\pi f_d\pi t + i\pi a_r t^2 + i\pi J_r t^3}, \end{aligned} \tag{26}$$

where c_1, a_1 and c_2, a_2 are quadratic rate and chirp rate of the respective chirps. Applying GTFT to $x^{recv}(t)$, we get:

$$X_{\alpha,\lambda}^{recv}(f) = \int_{-\infty}^{+\infty} rect\left[\frac{t-t_d}{\tau}\right]\Big[e^{ic_1\pi(t-t_d)^3+ia_1\pi(t-t_d)^2} + e^{ic_2\pi(t-t_d)^3+ia_2\pi(t-t_d)^2}\Big].e^{i2\pi f_d t+i\pi a_r t^2+i\pi J_r t^3} \cdot K_{\alpha,\lambda}(t,f)dt, \quad (27)$$

If $\lambda f_0^3 = c + J_r$, cubic phase term is zeroed out and we get:

$$= A_\alpha \int_{-\infty}^{+\infty} rect\left[\frac{t-t_d}{\tau}\right] exp\Big[i\pi[\cancel{ct^3} - ct_d^3 - 3ct^2t_d + 3ctt_d^2 + at^2 + at_d^2 - 2att_d + 2f_d t + a_r t^2 + \cancel{J_r \cdot t^3} - 2ft \quad (28)$$
$$\cdot \text{cosec}\alpha + t_0^2 f^2 \text{cot}\alpha + f_0^2 t^2 \text{cot}\alpha + \lambda t_0^3 f^3 - \cancel{\lambda t^3 f_0^3}\Big] dt,$$

where $A_\alpha = \sqrt{1 - i\cot\alpha}$. Thus, optimum λ (for each received wave) is obtained by cubic phase matching condition:

$$\lambda = \frac{c+J_r}{f_0^3} = \frac{(c+J_r).T_{max}^{3/2}}{f_s^{3/2}}. \quad (29)$$

Equation of optimum λ_1 and λ_2 corresponding to first and second chirp are given by

$$\lambda_1 = \frac{c_1+J_r}{f_0^3} = \frac{(c_1+J_r)T_{max}^{3/2}}{f_s^{3/2}}, \quad (30)$$

$$\lambda_2 = \frac{c_2+J_r}{f_0^3} = \frac{(c_2+J_r)T_{max}^{3/2}}{f_s^{3/2}}. \quad (31)$$

Optimum GTFT angle α is obtained using quadratic phase match condition in Eq. (28), so equation of optimum α_1 and α_2 corresponding to first and second chirp are given by:

$$\tan\alpha_1 = \frac{f_s}{T_{max}[3c_1t_d - (a_1 + a_r)]}, \quad (32)$$

similarly,

$$\tan\alpha_2 = \frac{f_s}{T_{max}[3c_2t_d - (a_2 + a_r)]}. \quad (33)$$

Thus, we can calculate a_r from Eq. (32) and Eq. (33). Considering Eq. (24) at two different optimum angles α_1, α_2 and matched λ_1, λ_2

$$\Delta d_{1n} = f_s t_d \cos\alpha_1 + (f_d + a_r t_d - 1.5c_1t_d^2)T_{max}\sin\alpha_1$$

$$\Delta d_{2n} = f_s t_d \cos\alpha_2 + (f_d + a_r t_d - 1.5c_2t_d^2)T_{max}\sin\alpha_2$$

f_d and t_d can be calculated from the above two equations with the use of the estimated acceleration parameter.

C. Double quadratic chirp waveform: Estimation error

The mean of the estimated parameters obtained by the separate Eqs. (29, 30) from each quadratic chirp is taken to reduce the parameter estimation error in J_r. Thus, we have:

$$J_r = \frac{f_o^3 \cdot (\lambda_1 + \lambda_2) - (c_1 + c_2)}{2}. \quad (34)$$

Estimation error in J_r is present due to errors in the estimated parameters i.e $\delta\lambda_1$ and $\delta\lambda_2$. Thus, δJ_r is estimation error in J_r defined as:

$$\delta J_r = \frac{f_o^3 \cdot (\delta\lambda_1 + \delta\lambda_2)\cdot}{2}. \quad (35)$$

Assuming $\delta\lambda_1$ and $\delta\lambda_2$ are independent Gaussian random variables $N(0,\sigma^2)$, variance in J_r is calculated as:

$$var(J_r) = \frac{\sigma^2 \cdot f_o^6}{2}. \quad (36)$$

We can calculate a_r and t_d from Eq. (31) or from Eq. (32) of paper. Thus, we get,

$$t_d = \frac{f_o^2 \cdot (\text{cot}\alpha_1 - \text{cot}\alpha_2) + (a_1 - a_2)}{3 \cdot (c_1 - c_2)}. \quad (37)$$

Error in t_d depends on the estimation errors of α_1 and α_2 i.e. $\delta\alpha_1$ and $\delta\alpha_2$ respectively. Assuming they are $N(0,\sigma^2)$ random variables, we get

$$var(t_d) = \frac{\sigma^2 \cdot f_o^4 \cdot (\text{cosec}^4\alpha_2 + \text{cosec}^4\alpha_1)}{9 \cdot (c_1 - c_2)^2}. \quad (38)$$

Similarly, we get,

$$a_r = \frac{f_o^2 \cdot (c_2 \cdot \text{cot}\alpha_1 - c_1 \cdot \text{cot}\alpha_2) + (a_1c_2 - a_2c_1)}{(c_1 - c_2)}, \quad (39)$$

and thus the error in a_r is

$$var(a_r) = \frac{\sigma^2 \cdot f_o^4 \cdot (c_1^2 \cdot \text{cosec}^4\alpha_2 + c_2^2 \cdot \text{cosec}^4\alpha_1)}{(c_1 - c_2)^2}. \quad (40)$$

The variance in f_d can also be calculated along similar lines. We take estimation errors in $u_1 = \Delta d_{1n}$ and $u_2 = \Delta d_{2n}$ i.e. δu_1 and δu_2 respectively as $N(0,\sigma^2)$ random variables. We get f_d as,

$$f_d = \frac{u_1 \cdot \text{cosec}\alpha_1 + u_2 \cdot \text{cosec}\alpha_2}{2 \cdot T_{max}} - \frac{f_s t_d \cdot (\text{cot}\alpha_1 + \text{cot}\alpha_2)}{2 \cdot T_{max}} - a_r \cdot t_d + 0.75 \cdot (c_1 + c_2) \cdot t_d^2. \quad (41)$$

Assuming error in t_d, a_r is negligible (for simplicity of calculation) while calculating variance in f_d, we obtain

$$var(f_d) = \frac{\sigma^2 \cdot (\text{cosec}^2\alpha_1 + \text{cosec}^2\alpha_2)}{(2 \cdot T_{max})^2} + \frac{\sigma^2 \cdot (u_2^2 \cdot \text{cosec}^2\alpha_2 \cdot \text{cot}^2\alpha_2 + u_1^2 \cdot \text{cosec}^2\alpha_1 \cdot \text{cot}^2\alpha_1)}{(2 \cdot T_{max})^2} + \frac{2f_s t_d \sigma^2 \cdot (u_1 \cdot \text{cosec}^3\alpha_1 \cdot \text{cot}\alpha_1 + u_2 \cdot \text{cosec}^3\alpha_2 \cdot \text{cot}\alpha_2)}{(2 \cdot T_{max})^2} + \frac{\sigma^2 \cdot (f_s^2 \cdot t_d^2(\text{cosec}^4\alpha_1 + \text{cosec}^4\alpha_2))}{(2 \cdot T_{max})^2}. \quad (42)$$

Thus, it is observed that the calculated error expressions, will be minimum, when the optimum fractional Fourier angles (α_1 and α_2) will be near to $\pm 90^0$.

D. MSE simulation: double quadratic chirp

Results of Monte Carlo simulation of 100 iterations for MSE of single target with t_d of $1sec$, f_d of $10Hz$, J_r of $2Hz^3$ and a_r of $5Hz^2$ using a double quadratic chirp are presented in Fig. (3). Here, double quadratic chirp $x^{tr}(t) = rect(\frac{t}{\tau})[e^{i(-20)\pi t^3+i(-110)\pi t^2} + e^{i20\pi t^3+i100\pi t^2}]$, is considered as transmitting waveform with pulse width of $1sec$. Input SNR is varied from -15 dB to 9 dB. The chirps are taken such that optimum fractional Fourier angle of first and second quadratic chirp in simulation are -86.56^0 and 86.56^0 respectively.

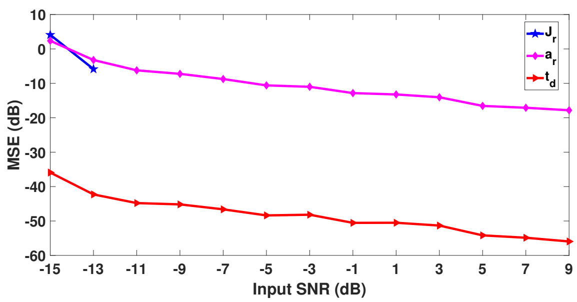

(a)

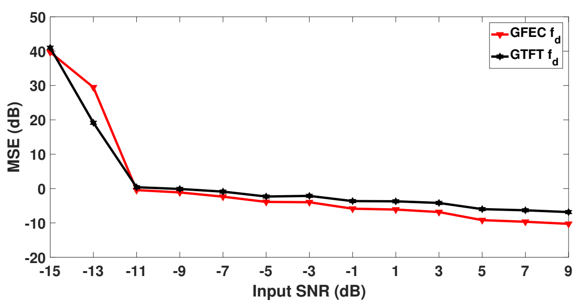

(b)

Fig. 3. MSE in estimation of a time delay and chirp offset parameters (a) MSE in estimation of J_r, a_r, and t_d (b) MSE comparison in estimation of f_d using GTFT and GFEC

V. Conclusion

In this paper, the SNR gain and impulse response of GFMF are derived. Simulations of SNR gain comparison are demonstrated to show the superior noise performance of GFMF as compared to time domain matched filtering, FrFT, and GTFT in the case of known time delay quadratic chirps. Simulation results are presented to show that GFMF gives lesser SNR degradation than time-domain matched filtering for non-zero Doppler frequency. The GFEC provides joint estimation of unknown time delay, frequency offset, frequency offset rate, and rate of frequency offset rate with a reasonable accuracy using double quadratic chirp waveform. Finally, the MSE of estimated parameters is presented, from which it can be inferred that the MSE of GFEC is lower compared to other existing methods for the same input SNR.

In the future, higher order waveforms can be analyzed using GFMF by appropriate selection of $h(\cdot)$ in the kernel. Higher order chirp waveforms can be used for joint estimation of target parameters using GFEC.

References

[1] S. Kumar and R. Saxena, "FrMF: Fractional Fourier matched filter," *Circuits, Systems, and Signal Processing*, vol. 37, no. 1, pp. 49–80, 2018.

[2] J. A. S. M. A. Richards and W. A. Holm, *Principles of Modern Radar: Basic Principles*. Raleigh, NC: Scitech Publishing, 2010.

[3] F. Zhang, R. Tao, and Y. Wang, "Matched filtering in fractional Fourier domain," in *2012 Second International Conference on Instrumentation, Measurement, Computer, Communication and Control*, 2012, pp. 1–4.

[4] F. Zhang, R. Tao, and Y. Wang, "Analysis and processing for chirp pulse with matched FRFT," in *2012 Second International Conference on Instrumentation, Measurement, Computer, Communication and Control*, 2012, pp. 5–9.

[5] X. Ning, L. Guo, and X. Sha, "Joint time delay and frequency offset estimation based on fractional Fourier transform," in *2012 International Conference on ICT Convergence (ICTC)*, 2012, pp. 318–322.

[6] H. Dexiu, Z. Huang, S. Zhang, and L. Jianhua, "Joint DOA, FDOA and differential Doppler rate estimation: Method and its performance analysis," *Chinese Journal of Aeronautics*, vol. 31, no. 1, pp. 137–147, 2018.

[7] S. B. Sahay, T. Meghasyam, R. K. Roy, G. Pooniwala, S. Chilamkurthy, and V. Gadre, "Parameter estimation of linear and quadratic chirps by employing the fractional Fourier transform and a generalized time frequency transform," *Sadhana*, vol. 40, no. 4, pp. 1049–1075, 2015.

[8] R. Tao, F. Zhang, and Y. Wang, "Fractional power spectrum," *IEEE Transactions on Signal Processing*, vol. 56, no. 9, pp. 4199–4206, 2008.